NDVI and a simple model of deciduous forest seasonal dynamics

Alicia K. Birky

School of Public Affairs, University of Maryland, College Park, MD 20742, USA

Abstract

Satellite derived NDVI for forest stands has been related to leaf area index (LAI) (Remote Sens. Environ. 61 (1997) 229), the fraction of absorbed photosynthetically active radiation (fPAR) (Remote Sens. Environ. 58 (1996) 115; Remote Sens. Environ. 61 (1997) 254) and to CO_2 uptake (Tellus 43B (1991) 188) with varying success. NDVI observations reflect leaf density, but are primarily indicators of process rates—photosynthesis and transpiration (Int. J. Remote Sens. 7 (1986) 1395). A simple model was developed of seasonal deciduous forest growth as a function of climate variables, including light intensity, temperature and moisture. The model was parameterized for six deciduous Maryland sites with non-photosynthetic biomass between 2.1 and 58.7 kgC/m^2. Model estimates of leaf biomass and gross primary productivity were compared to 1992 and 1993 1-km 10-day composite NDVI from the NOAA advanced very high resolution radiometer (AVHRR) instrument. Significant fluctuations in GPP appear to correlate to temporal variations in NDVI. A linear model relating NDVI to leaf biomass and specific gross primary productivity accounted for 51% of the variation in NDVI with *P*-values for all coefficients < 0.0001. Improvements in field data, more rigorous model treatment of cloud cover, consideration of site heterogeneity and corrections for atmospheric attenuation and satellite view angle might improve the correlation and thus allow use of NDVI for model calibration. © 2001 Elsevier Science B.V. All rights reserved.

Keywords: Forest; Seasonal; Biomass

1. Introduction

After years of heated debate, the scientific community has reached a general consensus on the reality of global climate change as a result of increased atmospheric concentrations of greenhouse gases. Carbon dioxide remains the primary focus and concentrations have increased by $>$ 25% over pre-industrial levels. Between 1980 and 1994, atmospheric CO_2 concentrations rose at an average annual rate of 0.4% (World Resources Institute, 1996). While the amount of atmospheric

CO_2 released from the combustion of fossil fuels is known accurately, our understanding of the complex interactions between terrestrial and marine ecosystems and the atmosphere on a global scale is limited. Therefore, scientific investigation of the process of carbon storage and release, particularly from soil and vegetation, is crucial to understanding the carbon cycle. Forests are known to play a significant role in the carbon cycle. While mature forests are believed to be neutral, steady state repositories of carbon, deforestation through clearcutting and biomass burn-

ing are a major source of CO_2 emissions—second only to fossil fuel combustion. Meanwhile, the reforestation of previously cleared land is a net carbon sink as organic matter is produced from photosynthesis. Furthermore, the feedback between atmospheric CO_2 concentrations and the rate of productivity, known as the CO_2 fertilization effect, is poorly understood and further complicates our ability to predict ecosystem response to greenhouse gas emissions. Thus, improving the accuracy and predictive power of forest models will increase our understanding of the global carbon cycle and allow for better informed policy decisions regarding CO_2 emissions and land use in light of global climate change threats.

1.1. Historic forest models

Historically, a number of approaches have been used to model tree and forest dynamics. Pipe models have been used to simulate biomass allocation to stem, bark, branches, large and fine roots, and foliage in individual trees (Mäkelä, 1997). Individual based gap models have been used to simulate successional forest dynamics in heterogeneous stands (Shugart and West, 1977). Complex population-based models simulating growth dynamics as a function of light, nutrients and water, have been applied to forest stands and are usually calibrated for homogenous, single species stands. Perhaps the most striking aspect of historic forest models and, even more so, of field and laboratory data, is the overwhelming attention to conifer species over hardwoods. Forest and tree dynamic models have been utilized primarily for forest management, specifically to predict and optimize tree growth for the forestry industry. However, in response to increasing regional and global environmental problems, scientific exploration of whole ecosystems has lead to the development of forest models within regional and large scale ecosystem models. A main objective of such studies is to investigate ecosystem dynamics and subsystem feedbacks, including climate, land use, population and competition dynamics.

1.2. Remote sensing

Field data has typically been used to correlate ecosystem models, but their increasing scale has made this approach time-consuming, expensive and often unfeasible for remote locations. Therefore, use of remote sensing data from aircraft and satellites for calibration and monitoring is becoming increasingly attractive. In addition, satellite remote sensing archives from the Landsat and NOAA projects provide the unique ability to calibrate models to historic temporal and spatial data. Several measures have been applied to remote sensing of vegetation, most of which rely on the reflectance properties of leaves in the visible and infrared wavelengths. High leaf pigment absorption, due to chlorophyll and carotenoids and thus, low reflectance occurs in the visible range 0.4–0.7 μm, also known as photosynthetically active radiation (PAR). Minimal absorption and high levels of spectral reflectance due to leaf scattering mechanisms occur in the near infrared range 0.74–1.1 μm and water spectral absorption occurs in the mid-infrared ranges between 1.1 and 2.5 μm (Tucker and Sellers, 1986). Due to coupling between the first and last of these phenomena, greenness indices focus on the upper portion of the visible range (VIS) and the near infrared (NIR), although various studies have used satellite data in narrow portions of all ranges. The normalized difference vegetation index (NDVI) has been applied extensively to primary productivity and remote sensing of biomass. The NDVI is calculated from the reflectance coefficients, a_i, in the upper visible and near infrared ranges:

$$NDVI = \frac{a_{NIR} - a_{VIS}}{a_{NIR} + a_{VIS}}$$

NDVI has been developed from both Landsat thematic mapper (TM) and NOAA AVHRR data. While the Landsat data offers higher spatial resolution (15–60 m) over AVHRR 1-km data, the advantage of the latter is the availability of free global, daily, continuous coverage. For AVHRR, NDVI is calculated from band 1 (0.58–0.68 μm) and band 2 (0.725–1.1 μm). Since the pathlength from the AVHRR instrument to the ground track pixel and illumination depend on

the satellite position at the time of imaging and since atmospheric moisture and cloud cover influence measurements, satellite data must be corrected. However, atmospheric effects and off-nadir observations have been shown to consistently reduce measurements of NDVI (Holben, 1986). Therefore, 10-day maximum composite images in conjunction with a cloud cover mask have been developed to reduce these effects. NDVI is calculated for each pixel for each day, then the maximum value over a 10-day period is selected on a pixel-by-pixel basis. At the time of this study, global 1-km NDVI 10-day composite images were available from NOAA for three periods each month beginning in April, 1992. The ratio, which falls between -1.0 and 1.0, is scaled and shifted to produce values between 0 and 200, with higher values indicating higher density of vegetation.

Tucker and Sellers (1986) point out that red and infrared reflectance observations provide information on surface chlorophyll density and, as such, are indicators of potential rates of photosynthesis and transpiration rather than leaf area index (LAI) or biomass. Under conditions of moisture or temperature stress, the chlorophyll density and stomatal openings are regulated to limit transpiration and, as a result, photosynthesis slows. In addition, leaf scattering and thus absorption would be reduced with the closure of stomata. Furthermore, in the absence of such stresses, but during cooler weather such as in the spring and fall, rates of photosynthesis may fall below potential rates indicated by chlorophyll density.

Fassnacht et al. (1997) reported disappointingly low correlation between remotely sensed vegetative indices, including NDVI and LAI for deciduous stands, though conifer stands produced more promising results with R^2 around 0.7 for most indices. The authors note findings that sensor signal saturates for LAI between 3 and 8, depending on the wavelength. Lüdeke et al. (1991) assert that for a pixel with complete forest cover, NDVI values reach a maximum of 0.8 for LAI near 3 and greater LAIs are not distinguishable with NDVI data. Mature deciduous forest stands reach LAIs much greater than 3 and for the Fassnacht study, all deciduous plots had seasonal maximum

LAIs > 4.4, possibly accounting for the lack of correlation. However, their results suggest improved correlation for multiple regressions involving several greenness indices and narrower (single color) bands within the visible region. At the same time, their data utilized a single date for remotely sensed data and litter-fall field data to estimate LAI and therefore, neglected temporal dynamics in productivity. Other studies have related NDVI to the fraction of absorbed photosynthetically active radiation (fPAR) (Veroustraete et al., 1996; Huemmrich and Goward, 1997) and to CO_2 uptake (Lüdeke et al., 1991).

2. Objectives

This study investigates the relationship between temporal NDVI variations and both productivity rates and leaf biomass as predicted by a simple model of seasonal carbon dynamics for North American deciduous forests. Quantifying this relationship would facilitate correlation of complex dynamic ecosystem models on large spatial scales using remote sensing data. Understanding the carbon cycle is of increasing importance as scientists seek to reduce the uncertainties in predictions of the effects and magnitude of human-induced climate change. The role of forest ecosystems as sources and sinks of carbon is especially important in this endeavor. Other potential applications of the relationship investigated here include the use of satellite archives to draw conclusions regarding the effects of current climate change processes and to quantify climate–biosphere feedbacks, such as the CO_2 fertilization effect. This study could also facilitate the use of remote sensing data to monitor ecosystem stress reflected by productivity rates.

3. Model

A simple model of forest growth and seasonal dynamics as a function of light intensity, temperature and moisture, was developed in STELLA4 on a PC platform. The model was initially based on the work of Janecek et al. (1989), with two

compartments representing green biomass (leaves, shoots and fine roots) and woody biomass (stem, branches and feeder roots). The model parameters and functional relationships were developed for an hourly time-step using the Euler method. In the interests of run-time, once the parameters were calibrated to Janecek's results for new growth oak stands, the relationships were simplified for 24-h averages to allow for a daily time-step. Since daily averages underestimate productivity and respiration due to diurnal light intensity and temperature variations, it was necessary to re-calibrate the parameters and functional relations to produce comparable results.

By using two state variables, a residual stock of green biomass remains after autumn leaf abscission to account for fine roots and storage. However, this approach yields photosynthetic activity during the winter, though at dramatically reduced rates due to cold temperatures and short days. The residual stock is necessary to allow for spring greening as temperatures and light intensity increase. To more closely simulate real systems, a third state variable was added to treat stored carbohydrates separately from green biomass. Thus, the green stock variable named LEAVES, accounts only for foliage, while the non-green stock variable, named R for 'rest', accounts for all non-photosynthetic material, including feeder and fine roots. Spring greening is simulated by the flow of carbon from the storage compartment (STOR) to the foliage compartment until photosynthetic activity exceeds storage flow. At this point, flow from the LEAVES into the storage compartment resumes at a low rate. Foliage production continues until stock levels approach the allometric relationship between green and non-green biomass. The switching function, described by Janecek et al. (1989), then determines allocation between non-photosynthetic biomass and foliage plus storage.

Finally, a moisture dependence function was added which reduces productivity during dry periods. Rainfall adds to the state variable MOISTURE, which serves as a marker for soil moisture. Soil moisture drydown is then simulated as a function of time and average air temperature, ceasing for extremely cold temperatures (≈ 200 K), reaching a nominal rate at 40 °F and doubling for average temperatures over 100 °F. From historic temperature data for Maryland, when daytime highs exceed 90–100 °F, daily average temperatures are $\approx 10°$ cooler.

The STELLA diagram of the resulting model is shown in Fig. 1. All stock variables and flows are quantified as kgC/m^2 with the assumption that tree biomass is $\approx 45\%$ carbon by dryweight. The model was run with Euler integration and daily timesteps with a 360-day year of 12 30-day months.

3.1. Production

Primary production is calculated as a product of three dependency functions—light, temperature, moisture—with the first two adapted from Janecek et al. (1989). To convert from an hourly formulation, average light intensity over daylight hours was calculated by integrating the function for daily variation given by Janecek. To simplify the calculation, attenuation due to atmospheric path-length was neglected. While this would tend to overestimate the average light intensity on the leaf surface, using an average intensity underestimates productivity due to feedbacks in accumulated leaf biomass. Therefore, this simplification creates insignificant error. The average was then assumed to apply over all daylight hours and was substituted into Janecek's Michaelis–Menton function as shown below:

$$h_1 = \text{DayLength} \frac{P_m}{k} \ln\left(\frac{KI + I_{ave}I_{max}}{KI + I_{max}e^{-k\text{LAI}}}\right)$$

$$\text{LAI} = u\text{LEAVES}$$

DayLength = number of daylight hours

$$= \left(\frac{24}{\pi}\right)\arccos[-\tan(\lambda)\tan(\delta)]$$

$\lambda = \text{latitude}$

$$\delta = \text{sun declination} = -0.408\cos\left[\frac{\pi}{180}(d+10)\right]$$

$d = \text{day number } (0-360)$

$$I_{ave} = \sin(\lambda)\sin(\delta) + \left(\frac{24}{\text{DayLength}\cdot\pi}\right)\cos(\lambda)\cos(\delta)\sin\left(\text{DayLength}\cdot\frac{\pi}{2}\right)$$

The values of the half-saturation parameter KI, the light intensity parameter I_{max} and the maximum productivity parameter P_m, were taken from Janecek and are listed in Table 1. The parameter u to convert from leaf mass in kg C to LAI is species specific and was set equal to 22 kg C^{-1} for a mixed deciduous stand. Due to the lack of firm data for the value of u, a sensitivity study was conducted with values from 10 to 30 in increments of 5. The model was highly sensitive for early season leaf biomass production. At 10, biomass prior to day 225 is less than half nominal (results for $u = 22$) and highly sensitive to temperature and moisture. Both storage and non-photosynthetic biomass levels at end of year are lower than the previous year. However, as u increases, the

Fig. 1. STELLA diagram.

Table 1
Model parameters

Name	Description	Value	Units	Source
Production				
P_m	Maximum production	0.00106	kg C/(m²h)	Oak (Janecek et al., 1989)
I_{max}	Maximum intensity of photosynthetically active radiation	640	W/m²	(Janecek et al., 1989)
K	Light absorption coefficient of a single leaf-layer	0.1	–	(Janecek et al., 1989)
U	Biomass to LAI conversion coefficient	22	$(kg\ C)^{-1}$	Best guess:
				Oak = 12 (Janecek et al., 1989)
				Oak = 22 (Whittaker and Marks, 1975)
				Norway spruce = 10 (Bossel and Shafer, 1989)
KI	Michaelis–Menton constant for production light dependence	150	W/m²	(Janecek et al., 1989)
Latitude	Geographic latitude of stand	38.5	Degrees	Southern Maryland
C	Production temperature dependence coefficient	609 000	K^{-1}	(Janecek et al., 1989)
Del_*H#*	Production temperature dependence coefficient	48 500	J/mol	(Janecek et al., 1989)
Del_*H*1	Production temperature dependence coefficient	176 000	J/mol	(Janecek et al., 1989)
Del_*S*	Production temperature dependence coefficient	557	J/(K mol)	(Janecek et al., 1989)
R_{gas}	Gas constant	8.314	J/(K mol)	(Van Wylen and Sonntag, 1986)
Allocation				
β	Allometric exponent	1.245	–	Calculated
θ	Allometric coefficient	37.4	$(kgC/m^2)^{1/\beta}$	Calculated
δ_x	Trajectory shaping parameter	1.0	–	Best guess
Respiration				
ω	Autotroph respiration temperature dependence parameter	0.06	K^{-1}	(Janecek et al., 1989)
τ	Autotroph respiration temperature dependence parameter	317	K	(Janecek et al., 1989)
a_{GA}	Maximum foliage respiration rate	0.108	d^{-1}	Oak (Janecek et al., 1989)
a_{RA}	Maximum nonphotosynthetic biomass respiration rate	0.005	d^{-1}	Best guess:
				Oak = 0.0072 (Janecek et al., 1989)
				Slash pine = 0.005/d (Cropper and Gholz, 1991)
				Norway spruce = 0.0007 (Bossel and Shafer, 1989)
γ	Respiring wood fraction parameter	0.45	–	(Janecek et al., 1989)
ϕ	Respiring wood fraction parameter	1.55	kgC/m²	(Janecek et al., 1989)
ψ	Respiring wood fraction parameter	1.218	kgC/m²	(Janecek et al., 1989)
Carbohydrate storage				
DL0	Minimum daylength for storage use	8	hours	Best guess
r_{max}	Maximum rate of storage use	0.06	kgC/d	Best guess
r_{sat}	Saturation constant for storage use	1.5	h^{-1}	Best guess
r_{loss}	Stochastic storage loss rate	0.00004	d^{-1}	Best guess
r_{stor}	Storage rate	0.0007	d^{-1}	Best guess

Table 1 (*Continued*)

Name	Description	Value	Units	Source
Litter, leaf abscission and other losses				
α	Maximum leaf abscission rate (fall)	0.24	d^{-1}	Best guess
ε	Leaf abscission parameter	2.1	h^{-2}	Oak (Janecek et al., 1989)
χ	Leaf abscission parameter	9.53	h	Oak (Janecek et al., 1989)
b_{GL1}	Leaf litter rate	24×10^{-8}	d^{-1}	Oak (Janecek et al., 1989)
b_{RL}	Nonphotosynthetic biomass litter rate	0.000028	d^{-1}	Best guess:
				Oak $= 4.8 \times 10^{-5}/d$ (Janecek et al., 1989)
				Norway spruce total deadwood loss $= 0.000028/d$ (Bossel and Shafer, 1989)
d_{GX}	Foliage loss from insects and disease	0.0001	d^{-1}	Best guess
d_{RX}	Woody biomass loss from insects and disease	0.00014–d_GX	d^{-1}	Best guess (Janecek et al., 1989)
Soil moisture				
d_{rate}	Nominal soil moisture drydown rate	0.05	d^{-1}	Best guess (calibrated to 37 °F)
d_{sat}	Drydown temperature dependence saturation rate	0.05	K^{-1}	Best guess
T_0	Temperature for drydown rate $= 0$	200	K	Best guess

maximum leaf biomass achieved rapidly saturates. At $u = 15$, leaf biomass reaches the same maximum as for $u = 22$, but 20 days later. Further increasing u causes earlier achievement of nominal maximum, then slightly larger late season leaf biomass. This indicates that model results are relatively insensitive to the value chosen for u within the range of 15–30.

To calculate the productivity temperature dependence, the average daily temperature was assumed to apply throughout each 24-h period. Since the 24-h average calculated from Janecek's assumed diurnal cosine variation was insignificantly different from the average of the 24-h high and low, the latter was applied in Janecek's temperature optimum shaping function, h_2:

$$h_2 = \frac{cT_{mm}e^{-\text{del}H\#/R_{gas}T_{mm}}}{(1 + e^{-\text{del}H1/R_{gas}\cdot T_{mm}})e^{\text{del}S/R_{gas}}}$$

where c, del$H\#$, del$H1$ and del$S$ are parameters as shown in Table 1 and R_{gas} is the universal gas constant. T_{mm} is the daily average temperature from climate data or for future predictions, a random number generated from historic mean and S.D. The function h_2 takes on values between 0 and 1 and scales production by 1.0 at 104 °F.

Kozlowski (1971) and Kramer and Kozlowski (1979) reported that internal water deficits and drought duration affect shoot growth, bud formation, leaf senescence and abscission, cambial growth and mid to late season wood production. However, leaf expansion appeared to be influenced more by water deficits during bud formation the previous season than drought during the expansion period. Seedling growth for 5-day watering intervals was observed to be half that of daily watering regimes. Therefore, a moisture dependence function was added to the model to simulate reduced production for soil moisture deficits. Since growth declines rapidly with decreases in water availability, the function was formulated as a sigmoid scaling factor which approaches 1.0 at a moisture measure of 0.1 inches and drops to 0.5 at 0.06 inches as shown below:

$$h_3 = \frac{1}{1 + 999\,e^{-0.155M}}$$

where $M =$ soil moisture, in 1/100 inch.

Production by the photosynthetic biomass flows directly into the LEAVES compartment and is calculated as:
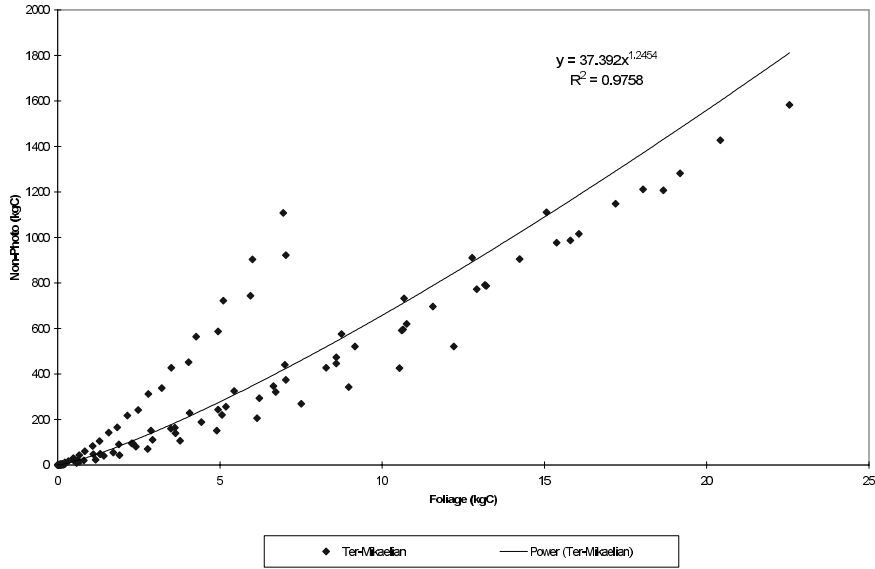
$$F_{assim} = h_1 h_2 h_3$$

Fig. 2. Allometric biomass relation. Relation fitted to data generated from equations for red oak, red maple, sugar maple, American beech, American Elm, white ash, yellow birch (Ter-Mikaelian and Korzukhin, 1997). Where not given, root biomass is estimated at 32% of above-ground biomass.

3.2. Partitioning

During the spring shooting phase, production of foliage is preferred over non-photosynthetic biomass. The transition to the secondary growth phase where new woody material is produced occurs as the stock of leaf biomass approaches the allometric relation:

$$R = \theta(\text{LEAVES} + \text{STOR})^\beta$$

Allometric partitioning of plant growth has been widely recognized and many studies have related stem, branch, root and leaf biomass to tree diameter at breast height (DBH). Ter-Mikaelian and Korzukhin (1997) documented biomass equations for 65 North American tree species based on 803 equations and nearly 50 studies. All equations were given in terms of DBH. The equations for eight deciduous species common to Maryland were selected and transformed to the form given above. A curve was then fitted to data points generated from these equations to produce a generalized allometric relation for deciduous forests, yielding $\theta = 37.4$, $\beta = 1.245$ with $R^2 = 0.976$, as shown in Fig. 2. Although individual species curves diverge with

increasing biomass and actual relationships would depend on species composition, this approach provides a reasonable approximation for mixed species stands.

To ensure continuous transition from the shooting to secondary growth phase, the growth trajectory in the LEAVES–R plane is assumed to follow an ellipse as it approaches the allometric relation, as described by Janecek et al. (1989). A switching function, S, determines the allocation of assimilate to the R compartment, such that the flow from LEAVES to R is:

$$F_{\text{GR}} = (1 - S)F_{\text{assim}}$$

where S is calculated as:

$$S = \begin{cases} 1 & \text{for } x \geq \Delta x + 1 \\ S_\sigma + \sqrt{(S_\sigma - 1)^2 - \left(\dfrac{S_\sigma - 1}{\Delta x}\right)^2 (x - \Delta x - 1)^2} & \text{for } 1 < x < \Delta x + 1 \\ S_\sigma & \text{for } x \leq 1 \end{cases}$$

where:

$$S_\sigma = \frac{F_{\text{assim}} + \dfrac{d\sigma}{dG}\sum F_{\text{LEAVES,out}} - \sum F_{R,\text{out}}}{\left(1 + \dfrac{d\sigma}{dG}\right)F_{\text{assim}}} \quad \text{for } F_{\text{assim}} > 0$$

$$\sigma = \theta(\text{LEAVES} + \text{STOR})^{\beta}$$

$$\frac{d\sigma}{dG} = \beta\theta(\text{LEAVES} + \text{STOR})^{\beta}$$

$$x = \frac{R}{\sigma}$$

where Δx is a constant parameter value determining the distance from the allometric relation where the transition to the secondary growth phase occurs in the LEAVES–R plane.

3.3. Respiration

Dark respiration is assumed over 24 h and the temperature dependency for both photosynthetic and non-photosynthetic biomass is taken from Janecek et al. (1989) as:

$$f(T) = e^{\omega(T_{\text{mm}} - \tau)}$$

where T_{mm} is the daily average temperature and ω and τ are as given in Table 1. Autotroph respiration for foliage is then:

$$F_{\text{GA}} = a_{\text{GA}} f(T)\text{LEAVES}$$

For the non-photosynthetic biomass, the fraction of living, respiring wood (RR) must be calculated. The fraction and the corresponding respiration are taken from Janecek et al. (1989) as:

$$\text{RR} = (R + \phi)^{\gamma} - \psi$$

$$F_{\text{RA}} = a_{\text{RA}} f(T)\text{RR}$$

Values used for the parameters a_{GA}, ϕ, γ, ψ and a_{RA} are given in Table 1.

3.4. Storage

Flow from the LEAVES compartment into storage (STOR) occurs at a constant percentage as long as productivity (F_{assim}) exceeds the flow available from STOR. However, when storage available for use exceeds photosynthesis, the difference between the two is drawn from storage to produce biomass and balance respiration. Using only the difference allows for a gradual decrease in reliance on storage use and prevents erratic state changes. The storage available for use depends on hours of daylight, thereby permitting use of storage if temperature or moisture stress occurs during the growing season. This formulation would also permit simulation of consumption stress due to insects, herbivores or logging. At the same time, storage use during the dormant season is suppressed. The flow from STOR to LEAVES (f_{stor}) is calculated as:

$$F_{\text{use}} = r_{\text{max}} fD\text{STOR}$$

$$fD = \frac{1}{1 + 999e^{-rsat(\text{DayLength} - \text{DL0})}}$$

IF ($F_{\text{use}} < F_{\text{assim}}$) THEN $F_{\text{stor}} = F_{\text{use}} - F_{\text{assim}}$

ELSE $F_{\text{stor}} = -r\_\text{stor}\text{LEAVES}$

where r_{max} r_{sat} DL0 and r_{stor} are constants with the values listed in Table 1. DayLength is calculated as shown above for the production function h_1. Parameters were calibrated to produce maximum storage levels in December, with flow into the LEAVES compartment beginning in March and minimum storage levels of around one third to half of winter levels occurring in May, as discussed by Kozlowski (1971).

3.5. Litter production and leaf abscission

Litter production from the non-photosynthetic compartment, R, occurs at a constant percentage as given by the parameter b_{RL}. Litter production from the LEAVES compartment also occurs at a constant percentage, but is augmented by leaf abscission in the fall. This latter phenomenon is triggered by decreasing hours of daylight, as calculated by the DayLength function defined above in the discussion of production functions. The formulation of Janecek et al. (1989) is used here, with the test for decreasing daylight determined by comparing DayLength for the current day to the previous day's calculation.

$$F_{\text{RL}} = b_{\text{RL}}R$$

$$F_{\text{GL}} = b_{\text{GL}}\text{LEAVES}$$

$$b_{GL} = \begin{cases} b_{GL1} + b_{GL2}(t) & \text{if } \dfrac{d\text{DayLength}}{dt} < 0 \\ b_{GL1} & \text{otherwise} \end{cases}$$

$$b_{GL2}(t) = \alpha \, e^{-\varepsilon(\text{DayLength} - \xi)^2}$$

Values for the litter production and leaf abscission parameters and their sources are given in Table 1. Leaf abscission parameters ε and ξ are taken from Janecek et al. (1989), but the value for α was selected to yield nearly 100% leaf loss within about 30 days.

3.6. Other losses

Storage, foliage and woody biomass losses due to insects, herbivores, disease and other stochastic events are included as constant percentage outflows from each compartment. Feedbacks between climatic stress, consumption and disease are neglected. The loss equations, in order of STOR, LEAVES and R are:

$$\text{loss} = r\_\text{loss}\text{STOR}$$

$$F_{GX} = d_{GX}\text{LEAVES}$$

$$F_{RX} = d_{RX}R$$

$$d_{RX} + d_{GX} = 0.00014 \; d^{-1}$$

The values for the loss rate parameters r_{loss}, d_{GX} and d_{RX} are given in Table 1.

4. Data

Sites for study were chosen from the Patuxent River watershed, which is a sub-watershed of the Chesapeake Bay. The watershed spans six Maryland counties and is influenced by the high-density human populations of Baltimore and Washington, DC. The more southerly locations are largely rural or forested. Dominant deciduous species include red maple, white oak, American elm and American beech.

4.1. Climate

Climate data was obtained from NOAA's National Climate Data Center (NCDC) by ftp from the web site ftp://ftp.ncdc.noaa.gof/pub/data. The station nearest the Patuxent watershed with historic data for 1991–1993 was located in Baltimore City. Data was obtained for daily rainfall in 1/100th inch and maximum and minimum temperatures in Fahrenheit. A daily average obtained from the maximum and minimum temperatures was applied to the model. To convert the climate data to a 360-day year, temperature data for the last day of a 31-day month was simply deleted. For months with 29 days, the last day's temperature was repeated. For 28-day months, the temperature on the first day of the succeeding month was also repeated. In order to not over- or under-predict growth due to rainfall, the rainfall of the last day of a 31-day month was added to the previous day's rainfall, while added days for months < 30 days were always assigned zero rainfall.

The climate data may account for some error in the model predictions due to location and data manipulation. For example, summer temperatures in Baltimore city probably exceed those in more remote forested sites due to heat island effects. However, winter temperatures may be milder and rainfall may be significantly different for those sites closer to the Chesapeake Bay. On the whole, the data should be generally representative of seasonal patterns and daily deviation from climate averages. Manipulation of the data to a 360-day year may shorten or lengthen drought and high-temperature stress periods as well as optimal growth periods. This effect should be slight and is accepted in order to simplify calculation of the day number, sun declination and day length.

4.2. NDVI

The US Forest Service's Forest Inventory and Analysis Database Retrieval System (http://www.srsfia.usfs.msstate.edulscripts/ewdbrs.htm) was used to locate 100% deciduous forest stands within the Patuxent watershed. Maryland data was only available for 1986. Due to time limitations, six sites were selected from an initial 53 representing above-ground non-photosynthetic biomass variations between 2.1 and 58.7 kgC/m², as described in Table 2. The latitude–longitude of these sites was used to select 1.1 km pixels of

Table 2
Data sites

Site ID	FIA age (years)	FIA site		FIA above ground biomass (kg/m^2)	Calculated			NDVI pixel	
		Longitude (°)	Latitude (°)		Non-photo biomass (kgC/m^2)	Foliage (kgC/m^2)	Initial storage (kgC/m^2)	Longitude (°)	Latitude (°)
5	25	76.4547	39.1111	17.09	10.16	0.35	0.07	76.4544	39.1108
16	45	76.6114	38.6111	37.96	22.58	0.67	0.13	76.6113	38.3608
24	85	76.6624	38.8333	47.98	28.54	0.80	0.16	76.6622	38.8330
30	25	76.7184	38.9444	3.53	2.10	0.10	0.02	76.7182	38.9442
54	45	76.8976	39.3333	77.06	45.84	1.18	0.24	76.8975	39.3330
58	65	76.9133	38.5000	98.63	58.66	1.44	0.29	76.9111	38.5000

10-day composite NDVI data, which was obtained by ftp from NOAA at http://grid2.cr.usgs.gov/ for April 1992–September 1993—the earliest data available. The scaled NOAA NDVI was shifted by 10 to allow for open water, dropped data and other data codes. The data was therefore corrected by subtracting 10 from the downloaded values. However, the scaling was retained, resulting in values between 98 and 176 for the six selected sites.

5. Results

The model functional results resemble those of the Janecek et al. (1989) model for the first 9 years of new growth, as illustrated in Fig. 3 for years 3–9, using the general deciduous parameters given in Table 1 with Maryland latitude and 1992 climate data. The magnitude of photosynthetic and non-photosynthetic biomass is greater than Janecek's results for Wisconsin, most likely due to more favorable climate conditions. To examine the correlation to NDVI data, the model was given initial conditions for each data location, including latitude, non-photosynthetic biomass and mid-winter carbohydrate storage. Total non-photosynthetic biomass was calculated from the FIA data, assuming that below ground biomass is 32% of above-ground biomass and that plant biomass contains 0.45 kg of carbon per kilogram dryweight. Growing season peak leaf biomass was calculated from the allometric relation discussed

Fig. 3. Model results for early growth.

above, using the parameters given in Table 1. Winter storage was then calculated as 20% of summer leaf biomass. The initial conditions shown in Table 2, along with zero leaf biomass, were used for model runs beginning January 1. Since actual storage depends mainly on climate conditions in the late summer and fall of the previous year, the model was run for 3 years using climate data for 1991–1993. Daily gross primary productivity (GPP) and leaf biomass predictions were recovered for April 1992–September 1993.

5.1. Correlation

As a first look at data correlation, the model results for 1992–1993 for site 16 were compared to the NDVI time series for the same period. In order to approximate the algorithm used to develop NDVI 10-day composites, a cloud-cover mask was applied to the model data, and maximum leaf biomass and GPP were selected for each 10-day period. Since cloud-cover information was not readily available, days with rainfall were eliminated from each period instead. Fig. 4 shows the comparison of 10-day masked maximum leaf biomass (L), gross primary productivity (GPP) and specific productivity (GPP/L) to the 10-day NDVI composites for site 16. The envelope of leaf biomass approximates the general shape of the NDVI, but is somewhat narrower. The model shows the shooting phase beginning the first week of March and leaf abscission in late October. The early and late greening shown in the NDVI may result from understory or herbaceous ground-cover effects. However, the bimodal appearance of the NDVI, with greater values in the early spring and fall than in midsummer, may indicate increased productivity during these periods. This would correspond to Kozlowski's observation that in many tree species, cambial growth slows or stops with midsummer droughts and as much as half the cambial growth occurs in the fall (Kozlowski, 1971).

Using ordinary least squares, NDVI was regressed on predicted GPP and leaf biomass data for all six sites according to the form:
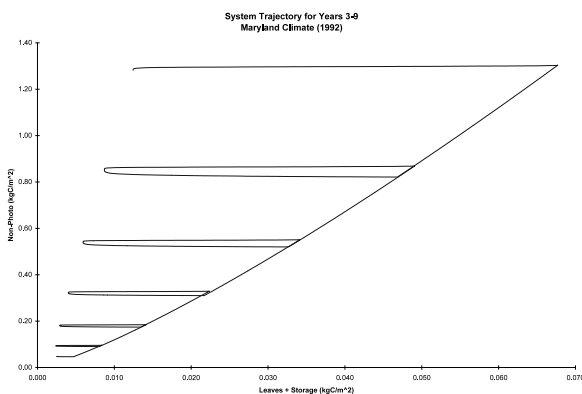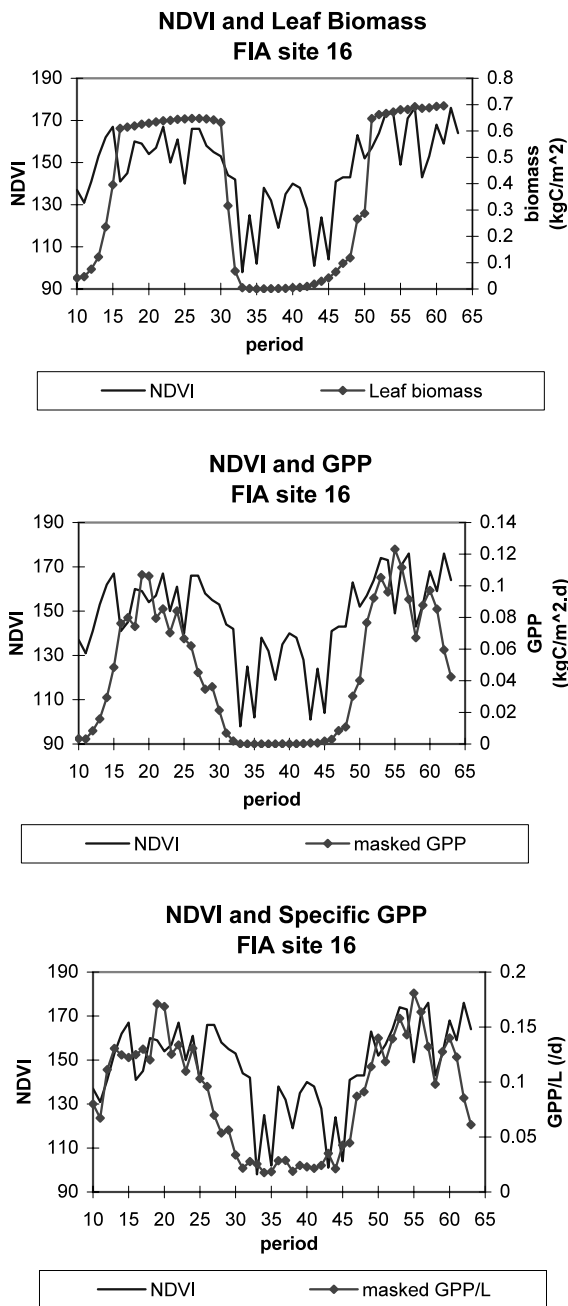
Fig. 4. Results for site 16.

$$\text{NDVI}_i = a + b_i(\text{leafbiom}_i) + b_2(\text{specificGPP}_i) + \varepsilon_i$$

$$\text{where: } \text{specificGPP} = \frac{\text{GPP}}{\text{leafbiom}}$$

A total of 324 observations were included. Plots of NDVI versus leaf biomass and GPP are shown in Fig. 5 and the regression results are given in Table 3. Leaf biomass and specific productivity together account for 51% of the variation in NDVI and all coefficients are statistically significant with P-values < 0.0001. The residuals are plotted in Fig. 6.

6. Discussion of results

Model predictions of temporal variations in specific productivity generally agree well with the seasonal NDVI observations. As shown in Fig. 4, modeled specific GPP captures spring green-up well and for the majority of the growing season for the 2 years, specific GPP and NDVI show corresponding peak and low values. Due to cool temperatures, specific GPP drops in the fall prior to leaf abscission. Meanwhile, NDVI values remain high until after leaf abscission, consistent with the hypothesis that NDVI measures potential rate of photosynthesis. This observation justifies the use of both specific productivity and leaf biomass in the statistical regression. The dynamic model accurately represents low productivity rates during temperature and moisture stress periods, particularly in early August 1993. Two notable exceptions occur around period 20 (11–20 July, 1992) and period 55 (1–10 July, 1993), where NDVI drops significantly but specific productivity predictions peak. These periods show favorable temperatures but relatively low soil moisture for both years.

It is likely that the simple, isolated model of soil moisture is inadequately accounting for drought stress, which could explain the July anomaly. The model does not incorporate soil characteristics, hydrology, or feedbacks from vegetation cover in predicting the drydown rate. It was intended that any correlation between soil moisture and NDVI would be captured in productivity rates. However, to investigate the adequacy of the model, predictions of soil moisture were tested as dependent variables in the statistical regression. Interestingly, this variable showed a statistically significant and negative correlation to NDVI. This effect is most

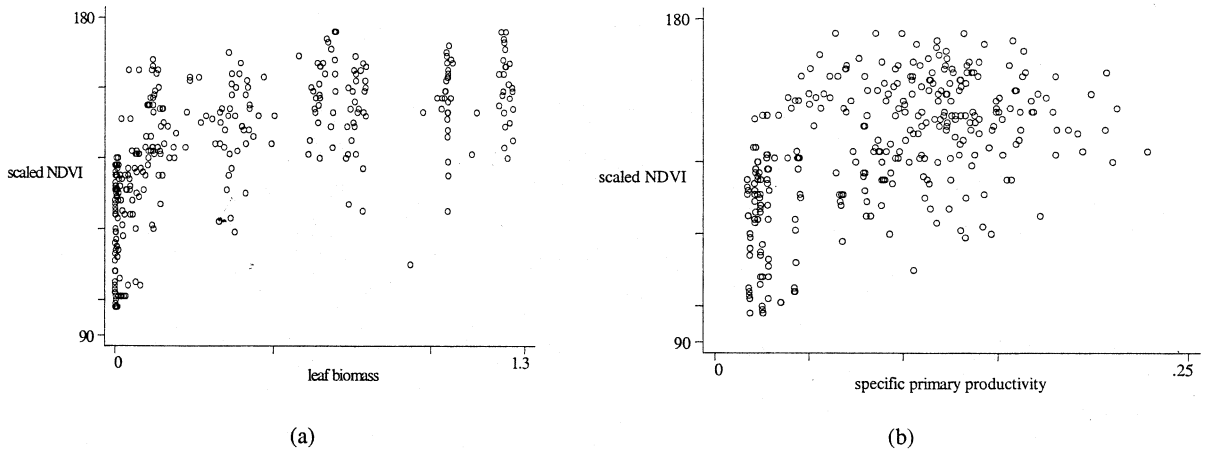(a)   (b)

Fig. 5. NDVI versus model predicted leaf biomass and specific productivity (all six sites).

Table 3
Regression results

NDVI	Coefficients		S.E.	t	$P > \lvert t \rvert$	[95% CI]	
Biom	b_1	22.24197	1.837388	12.105	0.000	18.62712	25.85681
Specgpp	b_2	143.0074	14.90204	9.596	0.000	113.6894	172.3254
Constant	a	121.6643	1.485506	81.901	0.000	118.7417	124.5868

Number of obs = 324; R-squared = 0.5142; $F(2,321) = 169.88$; Adj. R-squared = 0.5112; Prob $> F = 0.0000$; Root MSE = 13.169.

likely due to the covariation of soil moisture with other variables, notably the seasonal pattern of rainfall. For the study site, the majority of annual precipitation occurs in winter and early spring when low temperatures suppress productivity.

Other stress factors, such as disease and pests, are not included in the model and could account for the temporal discrepancies. In particular, gypsy moth caterpillars prefer oak—a dominant species in the study sites—and feed from early spring to mid-summer (June–July). It is notable that defoliation in New England and Mid-Atlantic States due to gypsy moth caterpillar infestations peaked in the early 1990s. F. William Ravlin of Virginia Polytechnic Institute's Department of Entomology reported that gypsy moths defoliated nearly 10 million acres nationwide in 1990 and nearly 800,000 acres of forest in Virginia in 1992 (Ravlin, 1998). Therefore, it is possible that the low July NDVI values reflect the impact of this pest.

Another potential source of error in the temporal variation of productivity is the lack of cloud-cover treatment in the model. Although maximum productivity values are eliminated from the comparison for days with rainfall, overcast days without rain are not. Including sunlight attenuation
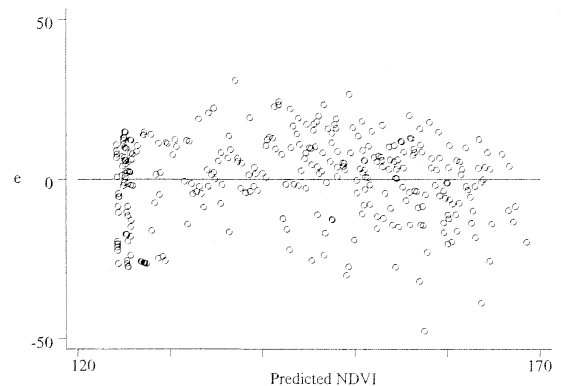

Fig. 6. Regression model residuals

due to clouds would reduce model productivity predictions, and could possibly mitigate these discrepancies. The NDVI data set includes the maximum measured value of the 10-day period and thus, should eliminate overcast days unless there is no satellite pass in the period with both a near-nadir and essentially cloud-free view. This latter possibility would also introduce a potential source of error and accounting for attenuation due to longer side-view pathlengths and atmospheric moisture would require a significantly more sophisticated algorithm than the simple 10-day maximum composite image used here. The lack of cloud cover treatment could also factor in the negative correlation between NDVI and model predictions of soil moisture, since high values of the latter would occur during and after precipitation and thus possibly during extended periods of cloud cover.

Although visual inspection of the temporal variation of NDVI with productivity demonstrates promising results, the statistical regression is less successful than anticipated. The regression model results in the following relation with $R^2 = 0.51$:

$$NDVI = 121.7 + 22.2(leafbiom)$$
$$+ 143.0(specificGPP)$$

where leafbiom is measured in kgC/m^2 and specificCGPP in d^{-1}.

The intercept term of 121.7 indicates the average background scaled NDVI and corresponds to a raw NDVI of 0.122. This result is comparable to bare soils of moderate brightness (0.12) and the value for bare soil of 0.128 achieved by Veroustraete et al. (1996). It should be noted that any reflectance due to snow cover is also included in the intercept term.

The bulk of the statistical significance shown is derived from the difference between winter and growing season values. Unfortunately, the correlation between peak growing season NDVI and spatial variations in biomass that is essential for ecosystem model calibration is not captured well in this study, as indicated by the fairly wide spread in the residuals (Fig. 6). As

noted, the dynamic model captures spring green-up and leaf abscission fairly well and this step function is the main contributor to the regression model coefficients. Examination of the NDVI data alone shows little variation in peak values among sites, despite FIA indications that these locations have very different quantities of aboveground woody biomass, as shown in Table 2. This lack of significant variation in remotely sensed data may contribute to the less than satisfactory results ($R^2 = 0.51$). This result also supports prior observations that satellite sensor readings saturate at leaf area indices well below those of mature forests (Tucker and Sellers, 1986; Lüdeke et al., 1991; Fassnacht et al., 1997).

By applying average values of species specific parameters, this study has neglected variations in species composition among the study sites. Variations in soil characteristics, and thus background reflectance, have also been neglected. In addition, 100% deciduous forest cover and heterogeneity within each 1 km pixel has been assumed. In order to minimize the error due to this assumption, study sites were selected from large forested plots reported by the FIA to be predominantly deciduous. However, the inaccuracy of the FIA data, particularly location information, adds considerable uncertainty to these results. Incorporating more reliable and finer resolution land cover and soil information and more complicated NDVI to LAI relations could improve site to site comparisons. For example, Lüdeke et al. (1991) include vegetated fraction and soil reflectance in the LAI to NDVI relation and demonstrate how the vegetated fraction can account for observed NDVI saturation values considerably lower than otherwise predicted.

These results suggest that while temporal variations in NDVI can be used as indicators of ecosystem stress, further work is required to quantify the relationships investigated here. It is possible that improving this model, or incorporating this representation of forest dynamics into more complex ecosystem models, will address the errors described above and improve the results.

7. Future work

Model predictions of seasonal variation in leaf biomass and productivity rates show promising correlation to temporal variation in NDVI. However, more work is needed to verify model predictions and improve the correlation of spatial variations in LAI and productivity to remotely sensed greenness indices. In particular, field measurements should be acquired to first correlate the model foliage predictions for varying aboveground biomass measurements, as well as yearly growth. Furthermore, the suggestion that multiple regressions against green, red, near and mid infrared and their ratios could produce improved correlations with deciduous LAI (Fassnacht et al., 1997) would be well worth investigating with field data and this model.

Improvements in the model formulation should be pursued as indicated by the potential sources of error discussed above. Components that should be investigated include light attenuation from cloud cover, hydrology and soil characteristics, vegetation feedbacks to soil moisture, pest infestations, site forest cover fraction and pixel heterogeneity. Finally, early spring and late fall NDVI values show slightly higher 'greenness' than is predicted by the model. This difference should be investigated, perhaps through inclusion of a herbaceous layer in the model.

References

Bossel, H., Shafer, H., 1989. Generic simulation model of forest growth, carbon and nitrogen dynamics, and application to tropical acacia and European spruce. Ecol. Model. 48, 221–265.

Cropper, W.P Jr, Gholz, H.L., 1991. In situ needle and fine root respiration in mature slash pine (*Pinus elliottii*) trees. Can. J. Forest Res. 21, 1589.

Fassnacht, K.S., Gower, S.T., MacKenzie, M.D., Nordheim, E.V., Lillesand, T.M., 1997. Estimating the leaf area index of north central Wisconsin forests using the Landsat Thematic Mapper. Remote Sens. Environ. 61, 229–245.

Holben, B.N, 1986. Characteristics of maximum-value composite images from temporal AVHRR data. Intern. J. Remote Sens. 7, 1417–1434.

Huemmrich, K.F., Goward, S.N., 1997. Vegetation canopy PAR absorptance and NDVI: and assessment for ten tree species with the SAIL model. Remote Sens. Environ. 61, 254–269.

Janecek, A., Benderoth, G., Lüdeke, M.K.B., Kindermann, J., Kohlmaier, G.H., 1989. Model of the seasonal and perennial carbon dynamics in deciduous-type forests controlled by climatic variables. Ecol. Model. 49, 101–124.

Kramer, P.J., Kozlowski, T.T., 1979. Physiology of Woody Plants. Academic Press, New York.

Kozlowski, T.T., 1971. Growth and Development of Trees, vol. 1 and 2. Academic Press, New York.

Lüdeke, M., Janecek, A., Kohlmaier, G.H., 1991. Modelling the seasonal CO_2 uptake by land vegetation using the global vegetation index. Tellus 43B, 188–196.

Mäkelä, A., 1997. A carbon balance model of growth and self-pruning in trees based on structural relationships. Forest Sci. 43, 7–23.

Ravlin, F.W., 1998. Gypsy Moth at Virginia Tech. Department of Entomology, Virginia Polytechnic Institute and State University web pages: http://www.gypsymoth.ento.vt.edu/

Shugart, H.H. Jr, West, D.C., 1977. Development of an Appalachian deciduous forest succession model and its application to assessment of the impact of the chestnut blight. J. Environ. Manag. 5, 161–179.

Ter-Mikaelian, M.T., Korzukhin, M.D., 1997. Biomass equations for sixty-five North American tree species. Forest Ecol. Manag. 97, 1–24.

Tucker, C.J., Sellers, P.J., 1986. Satellite remote sensing of primary production. Intern. J. Remote Sens. 7, 1395–1416.

Van Wylen, G.J., Sonntag, R.E., 1986. Fundamentals of Classical Thermodynamics. Wiley, New York.

Veroustraete, F., Patyn, J., Myneni, R.B., 1996. Estimating net ecosystem exchange of carbon using the normalized difference vegetation index and an ecosystem model. Remote Sens. Environ. 58, 115–130.

Whittaker, R.H., Marks, P.L., 1975. Methods of assessing terrestrial productivity. In: Leith, H., Whittaker, R.H. (Eds.), Primary Productivity of the Biosphere. Springer-Verlag, New York.

World Resources Institute, 1996. World Resources: A Guide to the Global Environment, 1996–97. Oxford University Press, New York.